Pharmacophore and k nearest neighbor studies on pyridazinylmethyl glucoside congeners derivative as potential antidiabetic agents

Mukesh Chandra Sharma◆

School of Pharmacy, Devi Ahilya Vishwavidyalaya, Indore-452001, Madhya Pradesh, India

Article Info	Abstract
	The article describes the development of a robust models and the investigation of structure activity relationship of forty one pyridazinylmethylphenyl derivatives reported for novel c-aryl glucoside SGLT2 inhibitors. 3D QSAR studies produced reasonably good predictive models with high cross validated correlation coefficient q2 (0.739) and external test set (0.708) values using the k nearest neighbor method. Pharmacophore model with lowest RMSD value (0.0653 Å) consists of aliphatic, hydrogen bond acceptor, hydrogen bond donor and aromatic feature was developed. The results of the present study may be useful in the design of more potent pyridazinylmethylphenyl derivatives as antidiabetic agents.

1. Introduction

Diabetes is a chronic metabolic disorder that is defined by the body's inability to generate insulin or the inability of the body to respond adequately to circulating insulin. Diabetes is acknowledged as one of the prevalent metabolic disorder affecting the global health and economy vigorously (Ain *et al.,* 2022).The World Health Organization (WHO) has foretold that the number of adults with diabetes by 2030 will have almost doubled worldwide, from 177 million in 2000 to 370 million (Duraisami *et al.,* 2021; Venkatachalam *et al.,*2021).There are two identified forms of diabetes; type 1 diabetes is distinguished as an autoimmune disease involving pancreatic β-cell, while type 2 diabetes is defined by β-cell dysfunction and insulin resistance (Dwarakanathan, 2006; Saltiel and Kahn, 2001). Diabetes and medications with allopathic drugs in long term can lead to many complications, damage, and dysfunction of various organs, especially the kidneys, liver, heart, and nerves (Gupta and Kori, 2022). Prediabetes is blood sugar level is higher than normal, but not high enough yet to be diagnosed as type-2 diabetes (Rani *et al.,* 2022). Sodium-dependent glucose cotransporters (SGLTs) couple the transport of glucose against a concentration gradient with the simultaneous transport of Na^+ down a concentration gradient (Mackenzie *et al.,* 1996). It is estimated that 90% of renal glucose reabsorption is facilitated by SGLT2 (Moe *et al.,* 1996). Two essential SGLT is forms have been cloned and identified as SGLT1 and SGLT2. SGLT1 is a high affinity, low-capacity transporter and therefore accounts for only a small fraction of renal glucose reabsorption (Evans

et al., 1985). Several therapeutic agents are available for monotherapy or for combination therapy with different mechanisms to treat diabetics, such as metformin, rosiglitazone, sitagliptine, acarbose, and glimepiride (Washburn, 2009). Over nearly a decade, a lot of different compounds have been reported as SGLT2 inhibitors as undergoing clinical trials. Phlorizin (Toggenburger *et al.,* 1982), serglifozin (Fujimori *et al.,* 2009) and remoglifozin (Fujimori *et al.,* 2008) are O-glycosides show strong inhibition of SGLT2 inhibitors. At present, dapagliflozin is the most advanced SGLT2 inhibitors in clinical trials (Phase 3) and canagliflozin is the second most advanced clinical candidate (Figure 1a). The quantitative structure activity relationship method attempts to link toxicity data with molecular descriptors derived from physicochemical properties or theoretical models of the molecular structure of chemical compounds (Toropov *et al.,* 2008). For achieving this aim and optimizing the pharmacophore requirement of pyridazinylmethylphenyl nucleus for design of potent and selective SGLT2 inhibitors, three dimensional studies k nearest neighbor molecular field analysis, and to obtain predictive models to guide the synthesis of novel antidiabetic agents.
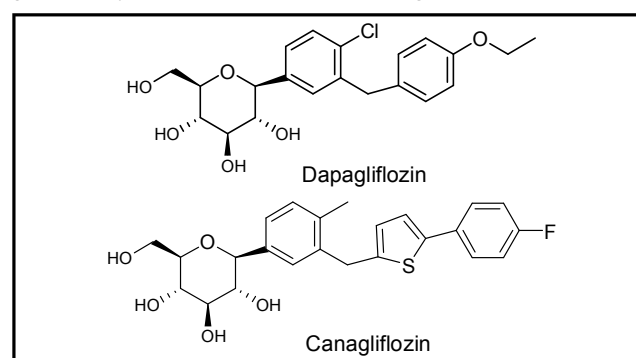
Corresponding author: Dr. Mukesh Chandra Sharma
Assistant Professor, School of Pharmacy, Devi Ahilya Vishwavidyalaya, Takshila Campus, Indore-452001, Madhya Pradesh, India
E-mail: drmukeshcsharma@gmail.com
Tel.: +91-9826372944

Figure 1(a): Dapagliflozin and canagliflozin
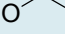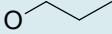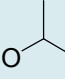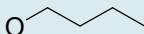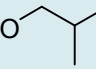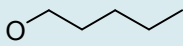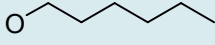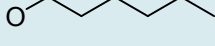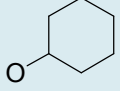
2. Materials and Methods
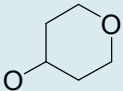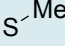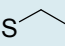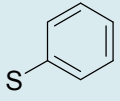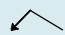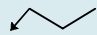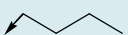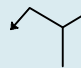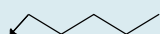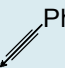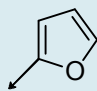
The biological data set was chosen from a series of forty one pyridazinylmethylphenyl derivatives as SGLT2 inhibitors reported (Kim *et al.*, 2010). The biological activity values IC_{50} (nM) reported in nanomolar units were converted to their molar units pIC_{50} and subsequently used as the dependent variable for the QSAR analysis. The converted to pIC_{50} for the analysis along with the structure of the compounds are given in Table 1. All the computational studies were performed by Vlife molecular design suite 3.5 (Vlife, 2004). All the structures of the compounds were drawn in 2D-APPL mode of software and exported to 3D model. Each compound was subjected to energy minimization and batch optimization using merck molecular force field, fixing root mean square gradients to 0.01 kcal/mol Å (Halgren, 1996). The sphere exclusion method (Golbraikh and Tropsha, 2002a) was adopted for division of training and test data set comprising of 31 and 10 molecules, respectively, with dissimilarity value of 8.8 where the dissimilarity value gives the sphere exclusion radius. The unicolumn statistics of the training and test sets are reported in Table 2. 3D QSAR models for the above data set are developed by using k nearest neighbor molecular field analysis method. Energy minimized and geometry optimized structure of molecules were aligned by the template-based method (Ajmani *et al.*, 2006) using VLife MDS software. The template structure, *i.e.*, pyridazinyl ring was used for alignment by considering the common elements of the series as shown in Figure 1b. The superimposition of all molecules based on minimizing root mean square deviation is shown in Figure 1c. To derive the k nearest neighbor descriptor fields, a 3D cubic lattice with grid spacing of 2 Å in x, y, and z dimensions was created to encompass the aligned molecules. The descriptors were calculated using a sp^3 carbon probe atom with a van der Waals radius of 1.52 Å and a charge of ± 1.0 with default cut-off energy value of ± 30 kcal/mol to generate steric and electrostatic fields (Clark *et al.*, 1989). This resulted in calculation of 6500 field descriptors for all the compounds in separate columns. The predicted r^2 was evaluated which is an indication of the predictive power of the model. The MolSign module in VLife MDS 3.5 provides tools for aligning small organic molecules based on their three dimensional pharmacophore features. Chemical features could be aromatic carbon centre; AlaC features (aliphatic), AroC feature (aromatic) hydrogen bond donor and acceptor, positive ionizable, charge interactions, and hydrophobic areas.
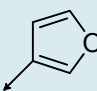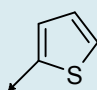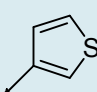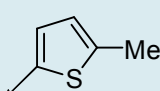
Table 1: Structure and biological activity of pyridazinylmethylphenyl derivatives SGLT2 inhibitors
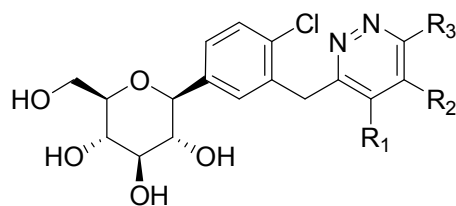
S. No.	R^1	R^2	R^3	IC_{50}	pIC_{50}	QSAR set
1	H	H	Cl	202	2.3057	Training set
2	H	H	(O-ethyl)	43	1.6332	Training set
3	H	H	(O-propyl)	70.8	1.8534	Test set
4	H	H	(O-isopropyl)	110	2.0412	Training set
5	H	H	(O-butyl)	109	2.0377	Training set
6	H	H	(O-isobutyl)	435	2.6381	Test set
7	H	H	(O-pentyl)	17	1.2343	Training set
8	H	H	(O-hexyl)	17.3	1.2388	Training set
9	H	H	(O-hexyl)	50.5	1.7036	Training set
10	H	H	(O-cyclohexyl)	111	2.0458	Test set

11	H	H	(tetrahydropyran-4-ol structure)	77.6	1.8893	Training set
12	H	H	S–Me	13.4	1.1271	Training set
13	H	H	S–ethyl	71.3	1.8536	Training set
14	H	H	phenyl–S	1870	3.2714	Test set
15	H	H	–Me	293	2.4668	Training set
16	H	H	(propyl)	131	2.1178	Training set
17	H	H	(butyl)	237	2.3742	Training set
18	H	H	(isopropyl)	259	2.4136	Training set
19	H	H	(pentyl)	356	2.5513	Test set
20	H	H	(isobutyl)	811	2.9097	Training set
21	H	H	(hexyl)	134	2.1272	Training set
22	H	H	≡–Ph	176	2.2451	Test set
23	H	H	(furan-2-yl)	64.3	1.8085	Training set
24	H	H	(furan-3-yl)	61.3	1.7879	Training set
25	H	H	(thiophen-2-yl)	71.4	1.8534	Test set
26	H	H	(thiophen-3-yl)	75.4	1.8772	Training set
27	H	H	(5-methylthiophen-2-yl)	168	2.2256	Training set
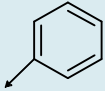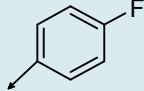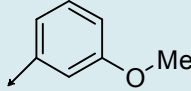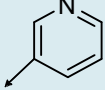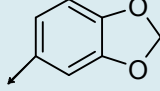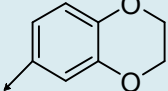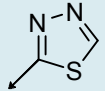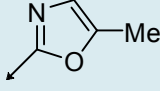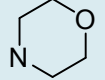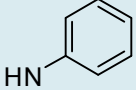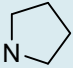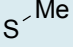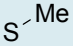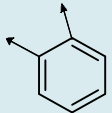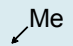
28	H	H		222	2.3463	Training set
29	H	H		272	2.4341	Test set
30	H	H		351	2.5456	Training set
31	H	H		64.9	1.8128	Training set
32	H	H		82.7	1.9173	Training set
33	H	H		103	2.0122	Test set
34	H	H		11.4	1.0561	Training set
35	H	H		1710	3.2327	Training set
36	H	H		700	2.8455	Training set
37	H	H		1140	3.0563	Test set
38	H	H		1040	3.0172	Training set
39	H	Me		1520	3.1816	Training set
40	Me	Me		10000	4.0000	Training set
41		H		10000	4.0000	Training set

Table 2: Unicolumn statistics of training and test set for 3D QSAR studies

Data set	Average	Max	Min	Std. Dev	Sum
3D-QSAR					
Training	2.3118	4.0000	1.0569	0.7191	76.2882
Test	2.0992	2.6385	1.2304	0.4988	16.7939

Table 3: The models developed by PCR regression analysis

	Equations
Model-1	pIC50=-0.03187-S_667 (-0.0472, -0.0387) +E_1147 (3.3422, 4.7377) + E_601(0.0669,0.5600)+E_1638(-0.2147, -2.6904) + H_692 (0.1419, 0.2158)
	Ntraining=31, Ntest=10, k Nearest Neighbour=4, Degree of freedom = 23, Optimum components=3, q2= 0.739, q2_ se = 0.186, F-test=27.54, pred_r2 = 0.708, pred_r2se = 0.198
Model-2	pIC50=0.6987-S_883 (-0.7443, -0.4992) +E_1141 (0.1006, 0.4681) +E_440 (-0.9070,-0.4739)
	Ntraining=31,Ntest=10, k Nearest Neighbour= 4, Degree of freedom = 23, Optimum components=3, q2= 0.6982, q2_ se = 0.4365, F-test=32.52, pred_r2 = 0.668, pred_r2se = 0.4268
Model-3	pIC50=0.8624+S_1015 (2.0685,3.7644)- E_1089 (-1.7220.-0.7370) +E_1491 (-0.1958, 0.2834) Ntraining=31,Ntest=10,k Nearest Neighbour =4,Degree of freedom = 27, Optimum components=3, q2=0.6874, q2_se = 0.5536, F-test=12.384, pred_r2 = 0.6523, pred_r2se = 0.5392
	Here, n represents number of observations, number of variables (k), DF is the degrees of freedom, squared correlation coefficient r2, regression, q2 is the cross-validated r2, and F is the F-statistic for the regression model. q2: Cross validated r2 (by leave-one-out method), q2_se: Cross validated standard error, pred_r2: Predicted r2 for external test set, pred_r2se: Standard error for predicted r2.

Table 4: Comparative observed and predicted activities (LOO) of pyridazinylmethylphenyl hSGLT2 inhibitors by 3D-QSAR models

Com	pIC$_{50}$	3D-Model-1		3D-Model-2		3D Model-3	
		Pred.	Res.	Pred.	Res.	Pred.	Res.
1	2.3057	2.1489	0.1568	2.1338	0.1719	2.5217	-0.216
2	1.6332	1.794	-0.1608	1.4879	0.1453	1.3829	0.2503
3	1.8534	1.8423	0.0111	1.7236	0.1298	1.4389	0.4145
4	2.0412	2.1635	-0.1223	2.2791	-0.2379	2.1978	-0.1566
5	2.0377	2.1137	-0.076	2.3236	-0.2859	2.4288	-0.3911
6	2.6381	2.1442	0.4939	2.6791	-0.041	2.2108	0.4273
7	1.2343	1.1692	0.0651	1.5295	-0.2952	1.5136	-0.2793
8	1.2388	1.5862	-0.3474	1.0427	0.1961	1.3184	-0.0796
9	1.7036	1.4713	0.2323	1.9815	-0.2779	1.7181	-0.0145
10	2.0458	1.9182	0.1276	2.1014	-0.0556	2.0114	0.0344
11	1.8893	1.6075	0.2818	1.7769	0.1124	1.7099	0.1794
12	1.1271	1.1808	-0.0537	1.3769	-0.2498	1.0146	0.1125
13	1.8536	1.7325	0.1211	1.5072	0.3464	1.5203	0.3333
14	3.2714	3.1108	0.1606	3.3136	-0.0422	3.4376	-0.1662
15	2.4668	2.2928	0.174	1.9359	0.5309	2.088	0.3788
16	2.1178	1.9683	0.1495	2.0521	0.0657	2.332	-0.2142
17	2.3742	2.0167	0.3575	2.1806	0.1936	2.5783	-0.2041
18	2.4136	2.2219	0.1917	2.8913	-0.4777	2.7455	-0.3319
19	2.5513	2.9273	-0.376	2.2576	0.2937	2.2129	0.3384

|							
20	2.9097	2.9052	0.0045	2.9427	-0.033	2.5678	0.3419
21	2.1272	2.0167	0.1105	1.9359	0.1913	2.2275	-0.1003
22	2.2451	2.408	-0.1629	2.4136	-0.1685	2.1617	0.0834
23	1.8085	1.9278	-0.1193	1.9896	-0.1811	1.8454	-0.0369
24	1.7879	1.6149	0.173	1.7014	0.0865	1.712	0.0759
25	1.8534	1.8906	-0.0372	1.8136	0.0398	1.6026	0.2508
26	1.8772	1.9372	-0.06	1.714	0.1632	2.0276	-0.1504
27	2.2256	2.5836	-0.358	2.3284	-0.1028	2.172	0.0536
28	2.3463	2.581	-0.2347	2.2383	0.108	2.1866	0.1597
29	2.4341	2.647	-0.2129	2.9139	-0.4798	2.2648	0.1693
30	2.5456	2.5851	-0.0395	2.2915	0.2541	2.3716	0.174
31	1.8128	1.5712	0.2416	1.8383	-0.0255	1.7399	0.0729
32	1.9173	1.8955	0.0218	1.8694	0.0479	1.8306	0.0867
33	2.0122	2.1988	-0.1866	2.1694	-0.1572	2.2995	-0.2873
34	1.0561	1.3133	-0.2572	1.0995	-0.0434	1.1851	-0.129
35	3.2327	3.1471	0.0856	2.9139	0.3188	3.0224	0.2103
36	2.8455	2.5064	0.3391	2.926	-0.0805	2.885	-0.0395
37	3.0563	3.0339	0.0224	3.293	-0.2367	3.2137	-0.1574
38	3.0172	3.1042	-0.087	3.1177	-0.1005	3.1608	-0.1436
39	3.1816	3.2491	-0.0675	2.8153	0.3663	2.9996	0.182
40	4.000	3.9267	0.0733	3.8407	0.1593	3.9216	0.0784
41	4.000	4.023	-0.023	3.9162	0.0838	3.9385	0.0615
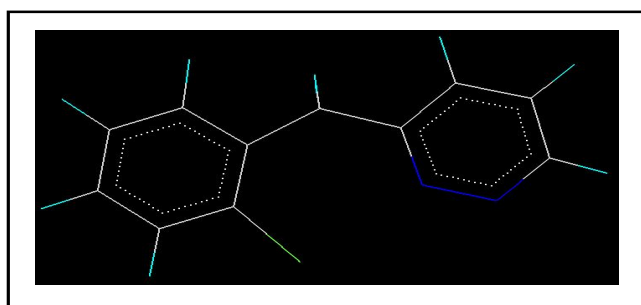
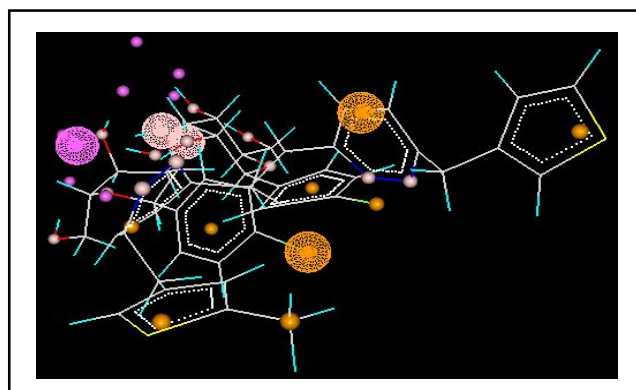**Figure 1(b): Pyridazinyl ring (template structure).**
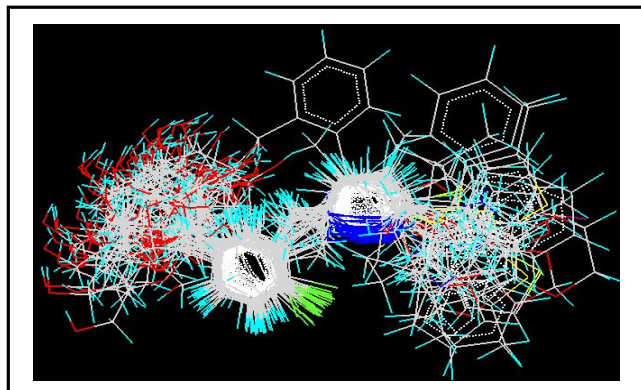

Figure 1(d): Selected pharmacophore.

Figure 1(c): Alignment of pyridazinylmethylphenyl derivatives.
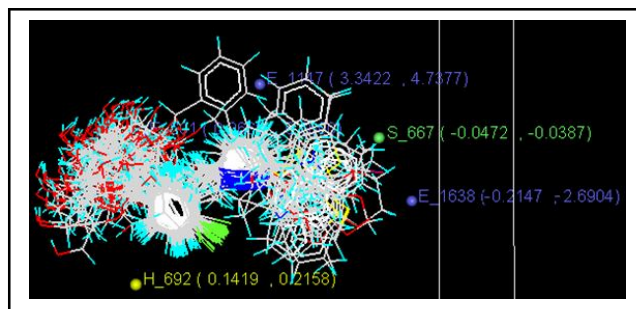

Figure 1(e): Contribution plot for steric, hydrophobic and electrostatic interactions model 1.
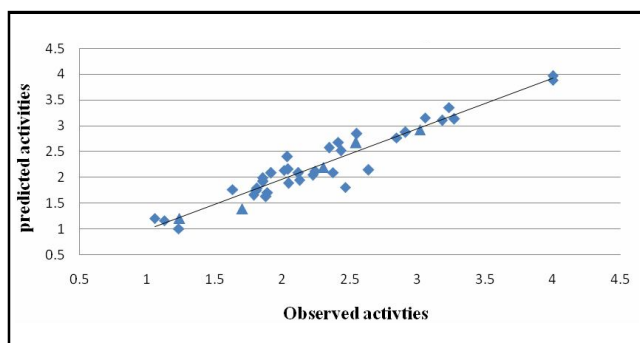
Figure 1(f): Plot of observed vs predicted activity 3D QSAR model 1 (♦-Training set, ▲-test set).
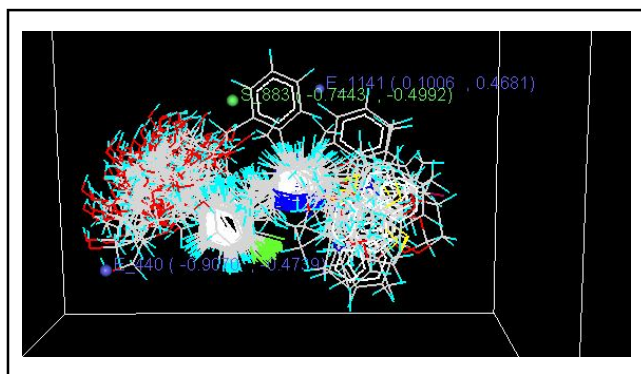

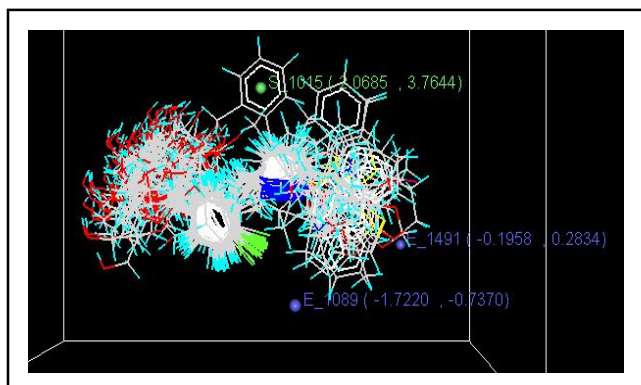**Figure 1(g): Contribution plot for steric and electrostatic interactions considering the model 2.**

Figure 1(h): Contribution plot for steric and electrostatic interactions considering the model 3.
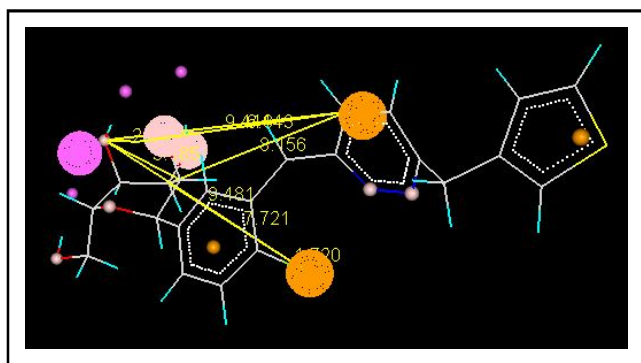

Figure 1(i): Distance best pharmacophore model.

3. Results

A series of pyridazinylmethylphenyl compounds with substitutions at R1, R2 and R3 position of pyridazinyl moiety are subjected to examine the relationships between structural modifications and activities against SGLT2 inhibitors with the help of molecular modeling. Three models are developed by simulated annealing (Zheng and Tropsha, 2000) and genetic algorithms variable selection (Holland, 1992) method coupled with principal component regression analysis. 3D model is considered to be predictive, if the following conditions are satisfied: squared correlation coefficient $r^2 > 0.6$, cross validated correlation coefficient $q^2 > 0.6$ and predictive $r^2 > 0.5$ (Afantitis *et al.,* 2009; Golbraikh and Tropsha, 2002b). Model-1 the template based alignment shows a q^2 (cross validated) of 0.7184 with 3D descriptors S_667 (-0.0472, -0.0387), E_1147 (3.3422, 4.7377), E_601 (0.0669, 0.5600), E_1638 (-0.2147, -2.6904) and H_692 (0.1419, 0.2158). The descriptors S_667, E_1147, E_601, E_1638 and H_692 are the steric, electrostatic and hydrophobic field energy of interactions between probe (CH_3) and compounds at their corresponding spatial grid points of 667, 1147, 601, 1638 and 692. Model-1 developed by simulated annealing method has a correlation coefficient (r^2) of 0.821, significant cross validated correlation coefficient (q^2) of 0.739, F test of 27.54, r^2 for external test set (predicted r^2) 0.708, coefficient of correlation of predicted data set 0.198.The 3D model 2 developed by simulated annealing method show predicts 82% of variance and is validated by an external set of compounds with a predictive correlation coefficient of 0.708. 3D data points S_883 (-0.7443, -0.4992), E_1141 (0.1006, 0.4681), E_440 (-0.9070,-0.4739) were generated that contribute to model 2, are shown in Figure 1e. The range was based on the variation of the field values at the chosen points using the most active molecule and its k nearest neighbor set. The external predictability of the above 3D model the test set was determined by predicted r^2, which is 0.668. So, the above results indicate that model for SGLT2 inhibitor generates 69 % and 67% internal and external model prediction, respectively. Molecular field analysis was applied for the generation of S_1015 (2.0685, 3.7644), E_1089 (-1.7220.-0.7370), E_1491 (-0.1958, 0.2834) steric and electrostatic descriptors based on aligned structures which shows good correlative and predictive capabilities. The model 3 developed by genetic algorithms gave 71% variance of prediction with correlation coefficient (r^2) of 0.7831, F test of 12.38, r^2 for external test set 0.6523, coefficient of correlation of predicted data set 0.5392 and degree of freedom 27. The result of the validation study is given in Table 3. The above model is validated by predicting the biological activities of the test molecules, as indicated in Table 4. The pharmacophore feature count, enter the value four, shows the minimum number of pharmacophore features generated for an alignment (Figure 1d). The tolerance field, enter the value 30 Å, shows the flexibility in percentage allowed while comparing two feature combinations across two molecules. For four point pharmacophore identification tolerance limit set up to 30 Å and max distance allowed between two features, set the value to 5 Å.

4. Discussion

Three best models are developed by simulated annealing variable selection and genetic algorithms method by considering 3D descriptors such as steric, electrostatic and hydrophobic parameters. From 3D model 1 (Figure 1e), it is observed that electrostatic descriptors E_1638 with negative coefficient are near from the R3

position of the pyridazinylmethylphenyl ring. This indicates that negative electrostatic potential is favorable for increase in the activity and more electronegative substituent group is preferred in that region. Most of the compounds (compounds 1, 29, 30, 35 and 37) with higher activity having electronegative substitution (chlorine, fluoro, methoxy groups) at the R3 position of pyridazinylmethylphenyl ring strongly support the above statement. The electrostatic interactions at the lattice point E_1147 and E_601 are also contributing positively, hence substitution of electron donating substituent R2 at the phenyl ring could increase activity. This indicates that electropositive groups are favorable on this site and presence of electropositive groups increases the activity of pyridazinylmethylp henyl compounds. Most of the compounds (compounds 13, 39, 40, 41) with higher activity having electropositive substitution at the R2 position of the pyridazinylmethylphenyl moiety strongly support the above statement. The positive values of electrostatic descriptors suggested the requirement of electropositive group like methyl, ethyl at the position of generated data point E_1147 and E_601 around pyridazinylmethylphenyl pharmacophore for maximum activity. In addition, more electropositive substituents are predicted to be beneficial near the R2 and R3, pyridazine ring. The presence of electropositive groups is also allowed near the pyridazine position 1, 2. The steric interaction fields represented in green lattice points at S_667 imply that the steric interaction along these lattice points are required to be addressed among which the interactions at S_667 are negatively contributing to activity. The presence of steric descriptor S_667 with negative values is also near from the R2 position of the ring which indicates that less steric or less bulky substituents are favorable on this site and presence of less steric substituents increases the activity of pyridazinylmethylphenyl compounds. Most of the compounds with having less bulky substitution at the R2 position of ring strongly support the above statement. The plots of predicted vs. observed values of pIC_{50} are shown in Figure 1f. The points generated in 3D-QSAR model 2 are S_883 (-0.7443, -0.4992), E_1141 (0.1006, 0.4681) and E_440 (-0.9070, -0.4739). Steric and electrostatic interaction field at lattice points 883, 1141, and 440, respectively, spread along as field points, the counter plot is shown in Figure 1g. 3D-QSAR studies helped to find out the importance of electropositive groups for biological activity. The electrostatic data point generated was E_1141 found that the electropositive groups like methyl, ethyl, propyl, isopropyl, and butyl were essential for potent activity and accordingly the substitutions were carried out for designing of new chemical entities. The presence of steric descriptor S_883 (-0.7443, -0.4992) with negative values is also near from the R1 position of the phenyl ring which indicates that less steric or less bulky substituents are favorable on this site. The presence positive values of steric descriptors suggested the requirement of sterically bulky groups at the R2 position of generated data point S_1015 (2.0685, 3.7644) near pyridazinylmethylphenyl pharmacophore for maximum SGLT2 inhibitors. From 3D QSAR model 3 (Figure 1h), it is observed that electrostatic descriptors like E_1089 (-1.7220.-0.7370) and E_1491 (-0.1958, 0.2834) are in the negative range near to R3 position of the moiety towards activity showing substitution of electronegative group in these sites enhances the activity. Further positive coefficient of the steric factor at S_1015 (2.0685, 3.7644) shows the substitution of a more bulky group in this region is preferable for the increase of activity. The obtained model contains aliphatic feature (AlaC) hydrogen bond acceptor (HAc) site, hydrogen bond donor (HDr)

site, and aromatic (AroC) region (Figure 1i). The distances between the pharmacophore sites were measured in order to confirm their significance to the activities. The average RMSD of the pharmacophore alignment of each two molecules is 0.0653 Å. These features for inhibitory activity are also highlighted through 3D space modeling approach which explored importance of critical inter-feature distances among the features in the pyridazinylmethylphenyl scaffold for SGLT2 inhibitors activity. The pharmacophore H-acceptor illustrates that H-bond acceptor groups are predicted to be beneficial near the pyridazine, in the para position in the R1 phenyl ring of compounds 8, 9, 10, 11. The distances among the various chemical features are as follows: Distance (1 HDr -1HAc) 2.9307 Å; Distance (1 HDr -1AroC) 9.4439; Distance (1HDr -1 AlaC) 9.4813 Å; Distance (1HAc -1AlaC) 7.7211 Å; Distance (2HAc-1 HDr) 3.1853 Å.

5. Conclusion

The k nearest neighbor region focusing model provided the most significant correlation of steric, electrostatic and hydrophobic fields with the SGLT2 inhibitors activities. In comparison to simulated annealing and genetic algorithms was found to provide a slightly better model. For example, compounds 1 and 29 which contain higher electronegative group Cl as the substituent R3 have higher activity than compounds 1-38 which contains lower electronegative atom. For another example, compounds 2-9 and 30 with the higher electronegative group OCH_3 at the R3 position. These new proposed compounds were generated by combining some less bulky, bulky and hydrophobic groups such as F, Br and I on and some electronegative groups like NO_2, OCH_3, F and Cl at R3 positions. Pharmacophore model was derived and best model include four features viz. hydrogen bond acceptor, hydrogen bond donor, aliphatic and aromatic group. QSAR studies of models parameters and k nearest neighbor region provided details of the structure activity relationship thus providing information regarding structural modifications with which to design new chemical entities analogue with better activity prior to synthesis.

Acknowledgements

Conflict of interest

The authors declare no conflicts of interest relevant to this article.

References

Ain, S.; Mishra, G.; Kumar, B.; Ain, Q. and Garg, R.K. (2022). Antidiabetic potential of developed solid lipid nanoparticles loaded with quercetin: *In vitro* and *in silico* studies. Ann. Phytomed., **11(2):**732-742.

Ajmani, S.; Jhadav, K. and Kulkarni, S.A. (2006). Three-dimensional qsar using the k-nearest neighbor method and its interpretation. J. Chem. Inf. Mod., **46:**24-31.

Afantitis, A.; Melagraki, G; Sarimveis, H.; Igglessi, M.O. and Kolliasnovel,G. A.(2009). A novel QSAR model for predicting the inhibition of CXCR3 receptor by 4-N-arryl-[1,4] diazepane. Eur. J. Med. Chem., **44:**877-884.

Clark, M.; Cramer, R.D. III and Van, O.N. (1989). Validation of the general purpose tripos 5.2 force field. J. Comput. Chem., **10:**982-1012.

536

Dwarakanathan, A. (2006) Diabetes update. J. Insur. Med., **38**(1):20-30.

Duraisami, R.; Sengottuvelu, S.; Prabha, T.; Sabbani, S.; Divya Presenna S. and Muralitharan, C.K. (2021). Evaluation of antidiabetic efficacy potency of polyherbal formulations in experimentally induced hyperglycemic rats. Ann. Phytomed., **10**(2):286-291.

Evans, L.; Grasset, E.; Heyman, M.; Dumontier, A.M.; Beau, J.P. and Desjeux, J.F. (1985). Congenital selective malabsorption of glucose and galactose. J. Pediatr. Gastroenterol. Nutr., **4**(6):878-886.

Fujimori, Y.; Katsuno, K.; Ojima, K.; Nakashima, I.; Nakano, S.; Ishikawa-Takemura, Y.; Kusama, H. and Isaji, M. (2009). Sergliflozin etabonate, a selective SGLT2 inhibitor, improves glycemic control in streptozotocin-induced diabetic rats and Zucker fatty rats. Eur.J. Pharmacol., **609**:148-154.

Fujimori, Y.; Katsuno, K.; Nakashima, I.; Ishikawa-Takemura, Y.; Fujikura, H. and Isaji, M.(2008). Remogliflozin etabonate, in a novel category of selective low-affinity sodium glucose cotransporter (SGLT2) inhibitors, exhibits antidiabetic efficacy in rodent models. J .Pharmacol. Exp. Ther., **327**:268-276.

Gasteiger, J. and Marsili, M. (1980). Iterative partial equalization of orbital electronegativity-a rapid access to atomic charges. Tetrahedron., **36**:3219-3228.

Golbraikh, A. and Tropsha, A. (2002a). Predictive QSAR modeling based on diversity sampling of experimental datasets for the training and test set selection. J. Comput. Aided. Mol. Des., **16**:357-369.

Golbraikh, A. and Tropsha, A. (2002b). Beware of q^2! J.Mol. Graphics. Mod., **20**:269-276.

Gupta, V. and Kori, M.L. (2022). Assessment of hepato and nephroprotective potential of polyherbal combinations against STZ-induced diabetic liver and kidney complications in wistar rats. Ann. Phytomed., **11**(1):311-319.

Holland, J.H. (1992). Genetic algorithms. Sci. Am., **267**:66-72.

Halgren, T.A. (1996). Merck molecular force field. II. MMFF94 van der Waals and electrostatic parameters for intermolecular interactions. J. Comp. Chem., **17**:520-552.

Kim, M.J.; Lee, J.; Kang, S.Y.; Lee, S.H.; Son, E.J.; Jung. M.E.; Lee, S.H.; Song. K.S.; Lee, M.; Han, H.K.; Kim, J. and Lee, J. (2010). Novel C-aryl glucoside SGLT2 inhibitors as potential antidiabetic agents: Pyridazinylmethylphenyl glucoside congeners. Bioorg. Med. Chem. Lett., **20**(11):3420-3425.

Mackenzie, B.; Loo, D.D.; Panayotova Heiermann,M. and Wright,E.M.(1996). Biophysical characteristics of the pig kidney Na+/glucose cotransporter SGLT2 reveal a common mechanism for SGLT1 and SGLT2. J. Biol. Chem., **271**(51):32678-83.

Moe,O.W.;Berry,C.A. and Rector,F.C.(1996). Renal transport of glucose. In: Brenner BM, ed.Brenner and Rector's the kidney, 5th edn.Philadelphia: WB Saunders, pp:375-415.

Saltiel, A.R. and Kahn, C.R. (2001). Insulin signalling and the regulation of glucose and lipid metabolism. Nature, **414**:799-806.

Toggenburger, G.; Kessler, M. and Semenza, G. (1982). Phlorizin as a probe of the small-intestinal Na^+,D-glucose cotransporter.A model. Biochim. Biophys. Acta., **688**:557-571.

Toropov, A.A.; Rasulev, B. F. and Leszczynski, J. (2008). QSAR modeling of acute toxicity by balance of correlations. Bioorg. Med. Chem., **16**:5999-6008.

Venkatachalam, T.; Chitra, M.; Kalaiselvi, P.; Chitra, A.; K. Sumathi, K.; Babu, S.; Senthilkumar, N. and Sattanathan, K. (2021). Phytochemical screening and antidiabetic potentiality of *Pavetta indica* L. (Angiosperms: Rubiaceae) methanol extract on streptozotocin induced diabetic mice. Ann. Phytomed., **10**(2):292-297

VLife MDS 3.5 (2004) Molecular Design Suite; VLlife sciences technologies Pvt. Ltd., Pune, India.

Rani,V.;Urvashi Nandal,U.; Reena and Sindhu,S.C. (2022). Nutrient milieu of products developed for prediabetic population using fenugreek seeds debittered by traditional techniques. Ann. Phytomed., **11(2):**344-350.

Washburn, W. N. (2009). Development of the renal glucose reabsorption inhibitors: A new mechanism for the pharmacotherapy of diabetes mellitus type 2. J. Med. Chem., **52**:1785-1794.

Zheng, W. and Tropsha, A. (2000). Novel variable selection quantitative structure-property relationship approach based on the k-nearest neighbor principle. J. Chem. Inf. Comput. Sci., **40**:185-194.